

In-situ synthesized $(\text{Al}_3\text{Zr} + \text{Al}_2\text{O}_3)_p/\text{A356}$ composites by direct melt reaction in Al-Zr-O system^①

ZHAO Yur-tao(赵玉涛), LI Zhong-hua(李忠华), CHENG Xiao-nong(程晓农),

DAI Qi-xun(戴起勋), CAI Lan(蔡 兰)

(School of Materials Science and Engineering, Jiangsu University, Zhenjiang 212013, China)

Abstract: A novel in-situ reaction system Al-Zr-O was developed. In situ Al_3Zr and Al_2O_3 particulate reinforced A356 alloy matrix composites have been fabricated by direct melt reaction method. The results show that the maximum sizes of Al_3Zr and Al_2O_3 particulates synthesized in the system $\text{ZrOCl}_2\text{-A356}$ are 1 μm and 3 μm respectively, and they are well distributed in the matrix. The investigation shows that the Al_3Zr crystal is in the shape of polyhedron and rectangle. There is a faceted growth phenomenon on Al_3Zr crystal surface. It is firstly found that the Al_3Zr crystal grows in the mechanism of twinning. The twinning plane is $(1\bar{1}4)$, and the twinning direction is $[2\bar{2}1]$. The crystal morphology of in-situ $\alpha\text{-Al}_2\text{O}_3$ particulate is rectangle or sphere. Furthermore, $(\text{Al}_3\text{Zr} + \text{Al}_2\text{O}_3)_p/\text{A356}$ composites have not only higher tensile strength at room temperature (376.2 MPa) but also higher yield strength (319.4 MPa) and higher tensile strength at elevated temperature (200 °C) than those of the A356 alloy. The dry sliding wear test shows that the wear resistance of the $(\text{Al}_3\text{Zr} + \text{Al}_2\text{O}_3)_p/\text{A356}$ composites is greatly enhanced with increasing particulate volume fraction.

Key words: in-situ synthesis; direct melt reaction; Al-Zr-O reaction system

CLC number: TB 331

Document code: A

1 INTRODUCTION

Recently, much attention has been paid to the development of effective fabrication processes for particulate reinforced metal matrix composites (PRMMC_s)^[1-3]. However, metal matrices reinforced with particles formed in situ are an emerging group of discontinuously reinforced composites that have distinct advantages over the conventional composites^[4,5]. In the in-situ fabrication process, the spontaneous reaction between the reactants is utilized to synthesize the reinforcements in the metal matrix. Especially, the direct melt reaction method (DMRM) is of simplicity, low cost and possibility of near net-shape forming and considered to be one of the most promising in-situ synthesis techniques of commercial production^[6]. In selecting a metal for fabricating the composites, aluminum (Al) can be noticed due to its lightmass, low melting point (933 K) and high processing. Up to now, however, in-situ reaction systems are mainly concentrated on Al-Ti-X, for example, Al-Ti-O, Al-Ti-B and Al-Ti-C. In-situ formed reinforcements are only focused on a few particles such as Al_3Ti , Al_2O_3 , TiB_2 , and TiC ^[7,8].

In this study, a novel in-situ reactive system Al-

Zr-O was developed. The novel $(\text{Al}_3\text{Zr} + \text{Al}_2\text{O}_3)_p/\text{A356}$ composites synthesized in the system Al-Zr-O was fabricated by the direct melt reaction between zirconium oxychloride with molten aluminum alloy A356. The dispersion behavior and crystal morphology of in situ formed reinforcements were studied. Moreover, the mechanical properties and dry sliding wear-resistance of the composite were investigated and the strengthening mechanism was discussed.

2 EXPERIMENTAL

Raw materials are Al-7Si-0.3Mg (A356) aluminum alloy ingot and zirconium oxychloride ($\text{ZrOCl}_2 \cdot 8\text{H}_2\text{O}$) powder (99.92%). Zirconium oxychloride was pre-heated to dehydrate the bounded water in it at 523 K for 3 h. Then the dried ZrOCl_2 was cooled, ground and screened. At the same time, 5 kg aluminum ingot was molten in a graphite crucible in an electric furnace under an argon atmosphere, and held at the experimental temperature of 1 073 K. Then dehydrated ZrOCl_2 power was added and incorporated by the melt-stirring method. During this stirring, in-situ Al_3Zr and Al_2O_3 particles were formed in the liquid aluminum and subsequently the melt was cast into

① **Foundation item:** Projects (2000156, 992B0007, 01KJB430003, JH02-039 and BE2002040) supported by the Ministry of Education of China, Economic Trade Commission of China, Science and Technology Commission of Jiangsu Province and Industry Key Project of Jiangsu Province

Received date: 2002 - 12 - 05; **Accepted date:** 2003 - 04 - 07

Correspondence: ZHAO Yur-tao, Professor, PhD; Tel: + 86-511-8791919, 8791292; E-mail: zhaoyt@ujs.edu.cn

a permanent mould.

The composite samples were cut off into discs ($d 10 \text{ mm} \times 5 \text{ mm}$) and polished for microstructure observation with the help of scanning-electron microscope (SEM), electron probe microanalysis (EPMA) and X-ray diffraction (XRD). The composite samples for transmission electron microscopy were sectioned into thin slices ($d 10 \text{ mm} \times 0.5 \text{ mm}$), mechanically ground on 1 000 grit silicon carbide paper, polished to approximately $60 \text{ }\mu\text{m}$ in thickness, and subsequently thinned using argon-ion beam at 5 kV, 4 mA at angles 30° and 10° . The foils prepared were carefully examined using JEM-2000EX transmission electron microscope equipped with a double-tilt holder and operated at 120 kV.

3 RESULTS AND DISCUSSION

3.1 Microstructure of composite

Fig. 1 shows the microstructure of the composite synthesized in the system $\text{Al}-\text{ZrOCl}_2$ using SEM and EPMA. It is indicated that the size of Al_3Zr particulate is in the range of $0.1 - 1.0 \text{ }\mu\text{m}$, whereas the size of Al_2O_3 particulate is in the range of $0.2 - 3.0 \text{ }\mu\text{m}$. In-situ formed Al_3Zr and Al_2O_3 particles are well distributed in the aluminum alloy A356 matrix.

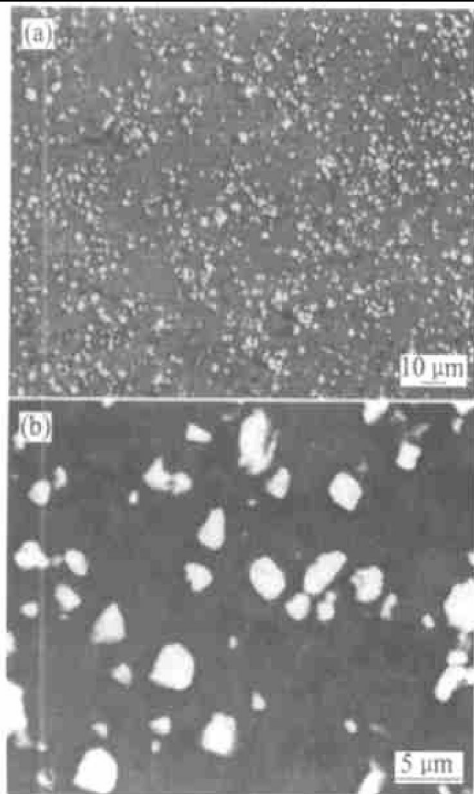


Fig. 1 SEM microstructure of $(\text{Al}_3\text{Zr} + \text{Al}_2\text{O}_3)_p/\text{A356}$ composites
(a) —SEM; (b) —EPMA

Fig. 2 shows the X-ray diffraction pattern of the composite synthesized by the direct melt reaction in the system $\text{Al}-\text{Zr}-\text{O}$. It is shown that the in situ

formed reinforcements in the system $\text{Al}-\text{Zr}-\text{O}$ are Al_3Zr and $\alpha\text{-Al}_2\text{O}_3$. The metallurgical reactions in the molten aluminum are as follows^[9]:

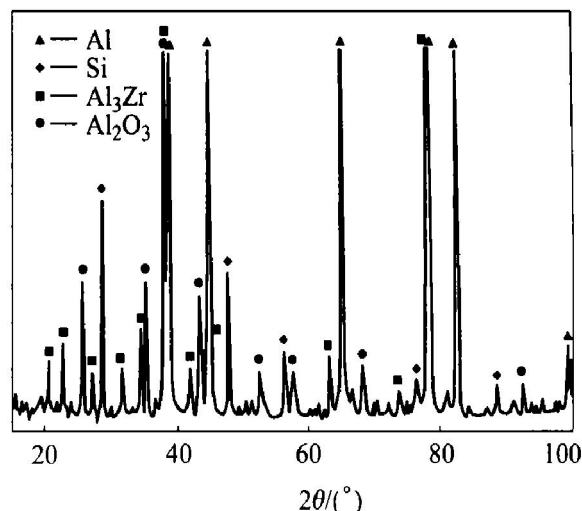
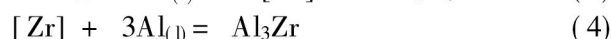
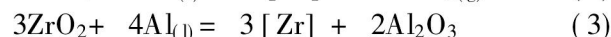
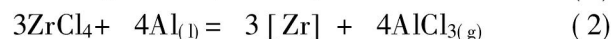
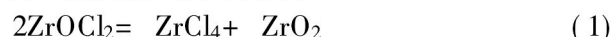


Fig. 2 X-ray diffraction pattern of composite synthesized in $\text{Al}-\text{Zr}-\text{O}$ system

3.2 Crystal morphology and growth

Figs. 3(a - d) show the crystal morphology and TEM diffraction pattern and growth model of Al_3Zr reinforcement. There are two forms of Al_3Zr crystal, one is polyhedral (Fig. 3(a)), the other is rectangular (Fig. 3(b)). The length/width ratio of the rectangle is in the range of $1.5 - 2.0$. There is a faceted growing tendency on the surface of the polyhedral and a twin growth on the surface of the rectangular. The interface between the Al_3Zr particulate and the Al matrix is smooth, clean and without reaction product. Moreover, the observation in many samples shows that the dislocation density of aluminum matrix near the polyhedral is higher than that of the matrix near the rectangular. The TEM diffraction pattern of the twin is shown in Fig. 3(c). According to the diffraction pattern, it is determined that the twin plane is $(1\ 1\ 4)$. The growth direction of the twin is $[2\ 2\ 1]$. The twinning growth model of the Al_3Zr crystal is illustrated in Fig. 3(d).

What is the relation between the twin and the morphology of Al_3Zr intermetallics? Depending on the experimental observation and the crystal growth theory^[10], the Al_3Zr intermetallic compound grows in the form of facet. The atomic arrangement on the interface of liquid/solid is smooth. Thus single molecule is difficult to accumulate up on the smooth surface of the Al_3Zr crystal. However, the twin occurs because of the atomic mismatch. It results in a very pronounced reentrant edge or groove. The diffusing Al_3Zr molecules

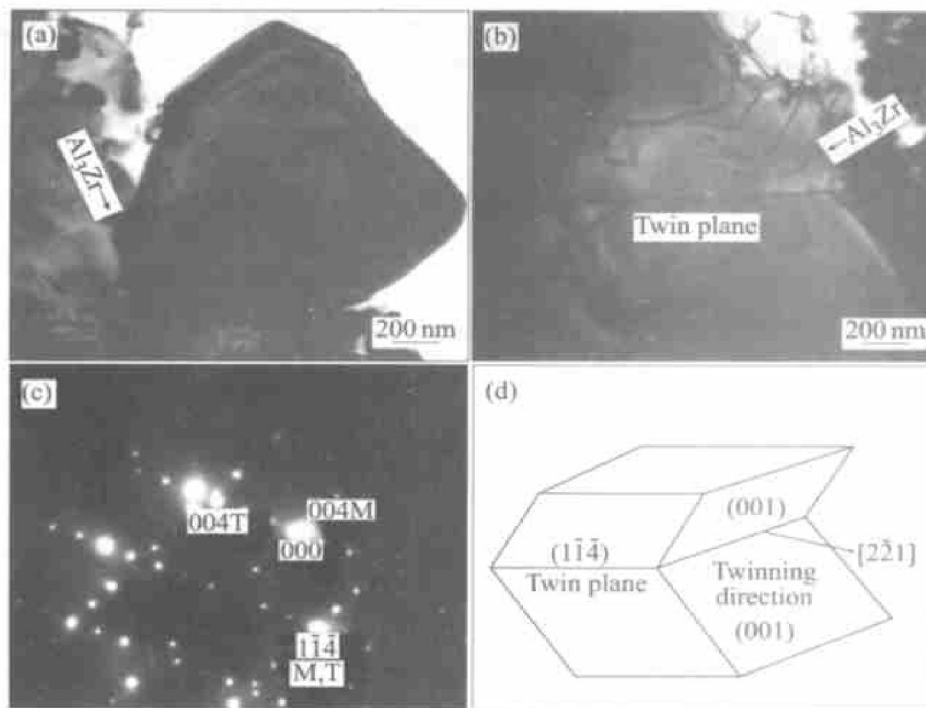


Fig. 3 Crystal morphology and growth model of Al_3Zr

(a) —Polyhedral Al_3Zr ; (b) —Rectangular Al_3Zr ; (c) —Diffraction pattern of twin;
(d) —Twinning model of Al_3Zr crystal

from the liquid melt are easy to attach to the groove. It may be concluded that the twin plane reentrant edge^[11], TP_{RE}, is important here for the growth kinetics of the Al_3Zr crystal. Although one twin can be observed in the Al_3Zr crystal, the fact is that there are four closely packed planes in the Al_3Zr crystal such as (114) , $(\bar{1}14)$, $(1\bar{1}4)$ and $(\bar{1}\bar{1}4)$ according to the analysis of the Al_3Zr crystal stereogram^[12]. The twinning phenomenon may take place on one or several closely packed planes. So it can result in one twin or several twins. Under the observation of the Al_3Zr morphology by SEM and TEM, the Al_3Zr reinforcement grows in the shape of rectangle when only one twin is caused, whereas the Al_3Zr reinforcement grows in the form of polyhedron when multiple twins are produced.

Figs. 4 (a–b) show the crystal morphology and TEM diffraction pattern of the Al_2O_3 particle. It is shown that the crystal morphology of the Al_2O_3 particulate is approximately equiaxial, and the Al_2O_3 crystal is of hexagonal structure.

3.3 Mechanical property of composite

The mechanical properties of the composite are shown in Fig. 5. The results indicate that the tensile strength and yield strength of the $(\text{Al}_3\text{Zr} + \text{Al}_2\text{O}_3)_p/\text{A356}$ composites are enhanced greatly with increasing volume fraction of particles. However, the percentage elongation of the composite is decreased with increasing volume fraction of particles. Furthermore, the $(\text{Al}_3\text{Zr}$

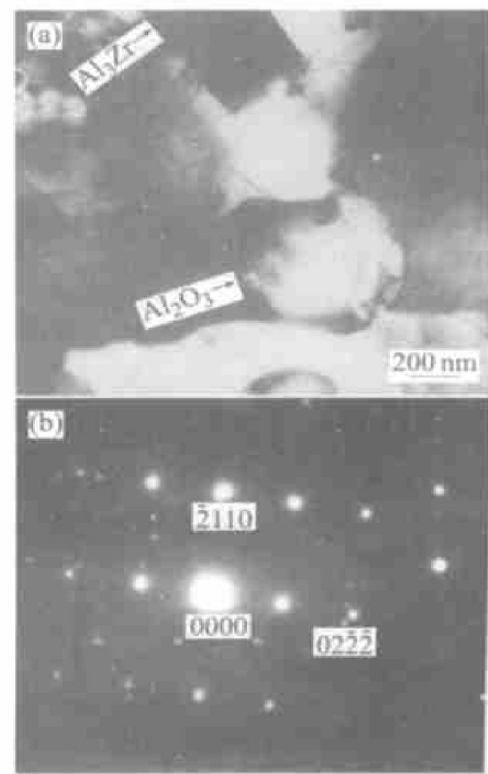


Fig. 4 Transmission electron micrographs of in-situ Al_2O_3 particulate

(a) —Equiaxial Al_2O_3 particulate;
(b) —Diffraction pattern of $[0\ 1\ 1\ 2]$

+ $\text{Al}_2\text{O}_3)_p/\text{A356}$ composites have higher tensile strength not only at room temperature ($\sigma_b = 376.2$ MPa) but also at elevated temperature ($\sigma_b = 187.6$ MPa) than those of

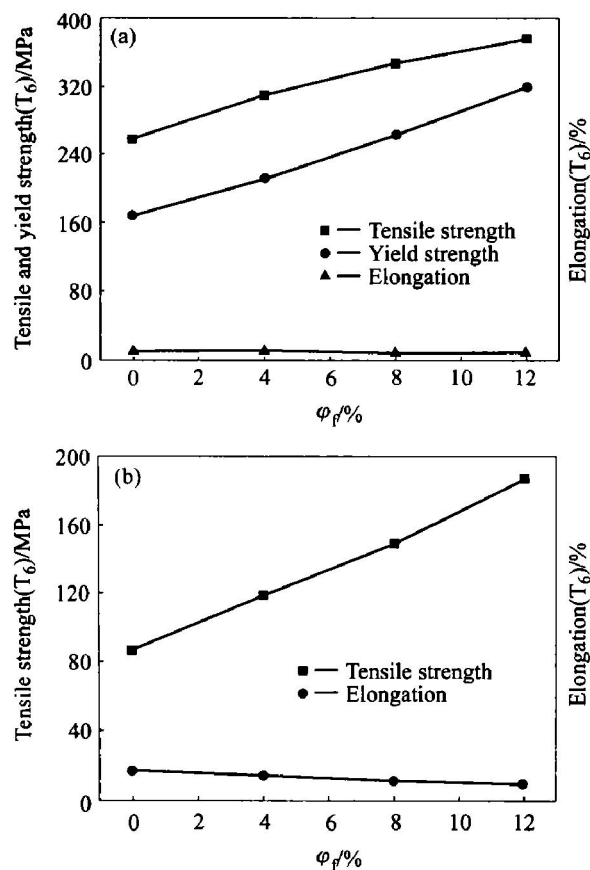


Fig. 5 Mechanical properties of $(Al_3Zr + Al_2O_3)_p/A356$ composites at room and elevated temperature
(a) —At room temperature;
(b) —At elevated temperature (200 °C)

A356 matrix alloy. The strengthening mechanism may include Orowan strengthening, grain-refined strengthening, and solid-solution strengthening^[13].

1) Orowan strengthening. Orowan strengthening results from the interaction between the dislocation and the dispersed particles. When the composite bears the load the plastic deformation of the material is caused. The hard Al_3Zr and Al_2O_3 particles act as obstacles to hinder the motion of dislocations near the particles in the matrix. The Orowan strengthening effect of the particles on the matrix is enhanced gradually with increasing particulate volume fraction.

2) Grain-refined strengthening. The experimental observations indicate that the Al_3Zr reinforcing phase can reduce the grain size of the aluminum matrix significantly. According to the analysis of the Al_3Zr crystal structure, the polyhedral Al_3Zr particles act as the heterogeneous nucleation catalyst for aluminum. The grain-refined strengthening effect of the Al_3Zr particulate is improved by increasing volume fraction of the polyhedral Al_3Zr particles.

3) Solid-solution strengthening. When a foreign Zr atom dissolves in the matrix Al, it may act as an atomic-sized obstacle to the motion of dislocations. Because the volume of the foreign Zr atom (0.023

272 nm³) is larger than that of the Al atom (0.016 603 nm³) a misfit strain field will be produced around the Zr atom that may interact with the dislocation strain field.

3.4 Wear property of composite

The dry sliding wear characteristics of the $(Al_3Zr + Al_2O_3)_p/A356$ composites is illustrated in Fig. 6. It is shown that the wear resistance of the $(Al_3Zr + Al_2O_3)_p/A356$ composites is superior to that of its matrix A356, and is greatly enhanced with increasing particulate volume fraction. The observation of the wear surface and subsurface by SEM shows that there are serious deformation and stripped pits on the wear surface of the A356 alloy, and the crack band occurs in the wear subsurface layer of the A356

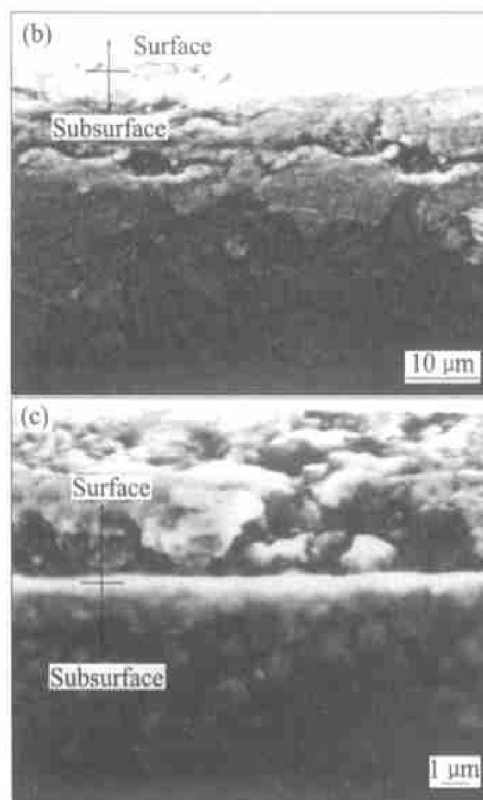
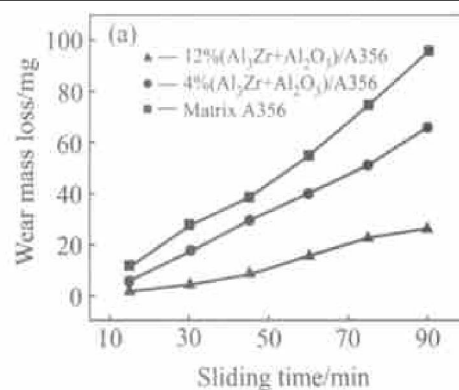


Fig. 6 Wear property and wear subsurface of $(Al_3Zr + Al_2O_3)_p/A356$ composites and matrix
(a) —Wear property of composites and matrix;
(b) —Wear subsurface of matrix A356;
(c) —Wear subsurface of composites

alloy. The wear feature of the matrix A356 is adhesive wear. However, the wear subsurface of the $(\text{Al}_3\text{Zr} + \text{Al}_2\text{O}_3)_p/\text{A356}$ composites has no cracks, the wear surface has also no severe wear and deformation. The wear feature of the $(\text{Al}_3\text{Zr} + \text{Al}_2\text{O}_3)_p/\text{A356}$ composites is abrasive wear.

4 CONCLUSIONS

1) In-situ Al_3Zr and Al_2O_3 particles reinforced aluminum alloy A356 matrix composites have been fabricated by the direct melt reaction in the system Al-Zr-O .

2) The crystal morphology of the Al_3Zr particulate with a tetragonal structure is mainly in the shape of polyhedral, whereas the crystal morphology of the Al_2O_3 particulate with a hexagonal structure is equiaxial.

3) It is found that the Al_3Zr crystal grows in the mechanism of twinning. The twinning plane is $(1\ 1\ 4)$. The twinning direction is $[2\ 2\ 1]$.

4) Tensile tests indicate that the $(\text{Al}_3\text{Zr} + \text{Al}_2\text{O}_3)_p/\text{A356}$ composites exhibit high strength not only at room temperature but also at elevated temperature. The wear resistance of the $(\text{Al}_3\text{Zr} + \text{Al}_2\text{O}_3)_p/\text{A356}$ composites is superior to that of the matrix A356 alloy.

REFERENCES

- [1] Ibrahim L A, Mohamed F A, Lavernia E J. Particulate reinforced metal matrix composites—a review [J]. J Mater Sci, 1991, 26: 1137–1156.
- [2] Mitra R, Chiou W A, Weertman J R, et al. Relaxation mechanisms at the interfaces in $\text{XD}^{\text{TM}} \text{Al/TiC}_p$ metal matrix composites [J]. Scripta Metall Mater, 1991, 25: 2689–2694.
- [3] Lloyd D J. Particle reinforced aluminum and magnesium matrix composites [J]. International Materials Reviews, 1994, 39(1): 1–23.
- [4] Wood J V, Davies P, Kellie J L F. Properties of reactively cast aluminum- TiB_2 alloys [J]. Mater Sci Tech, 1993, 9: 833–840.
- [5] Murthy V S R, Rao B S. Microstructural development in the directed melt-oxidized (DIMOX) Al-Mg-Si alloys [J]. J Mater Sci, 1995, 30: 3091–3097.
- [6] Nakata H, Choh T, Kanetake N. Fabrication and mechanical properties of in situ formed carbide particulate reinforced aluminum composite [J]. J Mater Sci, 1995, 30: 1719–1729.
- [7] TONG X C, FANG H S. Al-TiC composites in situ processed by ingot metallurgy and rapid solidification technology: part II. Mechanical behavior [J]. Metall Mater Trans A, 1998, 29A: 893–902.
- [8] Hashimoto S, Yamaguchi A, Yasuda M. Fabrication and properties of novel composites in the system Al-Zr-C [J]. J Mater Sci, 1998, 33: 4835–4842.
- [9] ZHAO Y T, SUN G X. In situ synthesis of novel composites in the system Al-Zr-O [J]. J Mater Sci Lett, 2001, 20(20): 1859–1861.
- [10] Lu S Z, Hellawell A. The mechanism of silicon modification in aluminum-silicon alloys: Impurity induced twinning [J]. Metall Trans A, 1987, 18A: 1721–1733.
- [11] Rath B B, Imam M A, Pande C S. Nucleation and growth of twin interfaces in fcc metals and alloys [J]. Mater Phys Mech, 2000(1): 61–66.
- [12] ZHAO Yur-tao, SUN Guo-xiong. Twin growth of in situ formed Al_3Zr in the system Al-ZrOCl_2 [J]. Chinese Journal of Materials Research, 2001, 15 (4): 420–424. (in Chinese)
- [13] ZHAO Yur-tao, SUN Guo-xiong. $\text{ZrAl}_{3(p)} + \text{Al}_2\text{O}_{3(p)}/\text{Al}$ composites fabricated by reaction in system Al-ZrOCl_2 [J]. The Chinese Journal of Nonferrous Metals, 2001, 11(1): 41–46. (in Chinese)

(Edited by PENG Chao-qun)